Interaction of atomic hydrogen with the β-SiC(100) 3×2 surface and subsurface

ARTICLE *in* THE JOURNAL OF CHEMICAL PHYSICS · OCTOBER 2007

Impact Factor: 2.95 · DOI: 10.1063/1.2799993

Interaction of atomic hydrogen with the β-SiC(100) 3×2 surface and subsurface

M. D'angelo,[a] H. Enriquez, N. Rodriguez, V. Yu. Aristov,[b] and P. Soukiassian[c]
Laboratoire SIMA, DSM-DRECAM-SPCSI, Commissariat à l'Energie Atomique, Saclay, Bât. 462, 91191 Gif sur Yvette Cedex, France and Département de Physique, Université de Paris-Sud, 91405 Orsay Cedex, France

A. Tejeda[d] and E. G. Michel
Departamento de Física de la Materia Condensada, Universidad Autónoma de Madrid, 28049 Madrid, Spain and Laboratoire SIMA, DSM-DRECAM-SPCSI, Commissariat à l'Energie Atomique, Saclay, Bât. 462, 91191 Gif sur Yvette Cedex, France

M. Pedio, C. Ottaviani, and P. Perfetti
ISM-CNR, Via del fosso del cavaliere 100, 00133, Roma, Italy and Elettra Sincrotrone Trieste, 34012 Basovizza, Italy

(Received 1 June 2007; accepted 25 September 2007; published online 29 October 2007; publisher error corrected 1 November 2007)

We investigate clean and atomic hydrogen exposed β-SiC(100) 3×2 surfaces by synchrotron radiation-based Si $2p$ core-level photoemission spectroscopy. The clean 3×2 surface reconstruction exhibits three surface and subsurface components. Upon hydrogen exposures, those surface and subsurface components are shifted to lower binding energies by large values, indicating significant charge transfer to the surface and subsurface regions, in excellent agreement with the recently discovered H-induced β-SiC(100) 3×2 surface metallization. In addition, the interaction of hydrogen results in a large reactive component at Si $2p$ supporting an asymmetric charge transfer in the third plane below the surface, in agreement with previous experimental investigations. However, the results are inconsistent with recent *ab initio* theoretical "frozen" calculations predicting H atom to be in a bridge-bond position. © *2007 American Institute of Physics*. [DOI: 10.1063/1.2799993]

I. INTRODUCTION

Because it is the smallest and simplest element in the Mendeleev classification, hydrogen plays a special role in surface/interface science. Together with other molecular adsorbates, it has been widely used to probe and/or selectively modify surface/interface properties.[1–8] This aspect is particularly important for semiconductor surfaces from both fundamental and applied points of view.[1–8] For instance, H atoms have been used to decorate Si dangling bonds forming either monohydride 2×1 or 1×1 Si(100) surfaces or achieving ideal nonreconstructed 1×1 surfaces on the Si(111) surface.[3,4] These features have resulted in the successful use of H in Si surface passivation.[2,5,7] In the latter case, ideal H-terminated 1×1 Si(111) or H/Si(100) surfaces have been found to remain totally inert even in air.[2,5,7] Molecular hydrogen has been shown to interact with the Si-terminated β-SiC(100) $c(4\times2)$ surface at sticking probabilities eight orders of magnitude higher than on silicon surfaces and efficient molecular dissociation leading to have H atoms also decorating the top-surface Si dangling bonds.[8] In strong contrast, the Si-rich β-SiC(100) 3×2 surface reconstruction remains totally inert to molecular hydrogen.[8] This very selective interaction of hydrogen molecules with these two very different surface reconstructions has been explained in terms of interdimer versus intradimer adsorption sites.[9] Another very interesting and useful aspect in nanoscience of H on semiconductor surfaces is the possibility of selectively removing groups of H atoms from a hydrogen-covered Si(100) surface using scanning tunneling microscopy (STM) as a tool.[10–12] This leads to the routine fabrication of nanostructures having very different reactivities from the surrounding surface (e.g., for oxidation or metallization).[10–12] In addition, Si hydrogenated surfaces with H atoms removed from one side of the dimer row lead to Si dangling bond wires for which conductivity has been predicted.[13–17]

Silicon carbide (SiC) is a IV-IV compound wide-band-gap semiconductor having a strong interest in high power, high temperature, high frequency, and high voltage microelectronic devices and sensors.[18–20] In addition, SiC exists in ultrahigh quality large wafer[21,22] and is one of the best biocompatible materials, a useful feature for interfacing with biology.[18,19] The (100) face of cubic silicon carbide (β-SiC) is made of alternating Si and C planes resulting in many different surface reconstructions (up to 9) ranging from Si-rich to C-rich surfaces.[23–25] Unlike silicon, germanium, or diamond, SiC is not a fully covalent semiconductor with a

[a]Present address: Institut des NanoSciences de Paris, Université Pierre et Marie Curie, 75251 Paris, France.
[b]On leave from Institute of Solid State Physics, Russian Academy of Sciences, Chernogolovka, Moscow district 142432, Russia.
[c]Also at Department of Physics, Northern Illinois University, Dekalb, IL 60115-2854. Electronic mail: patrick.soukiassian@cea.fr
[d]Present address: Matériaux et Phénomènes Quantiques, CNRS, Université Denis Diderot, BP 7021, 75205 Paris, France.

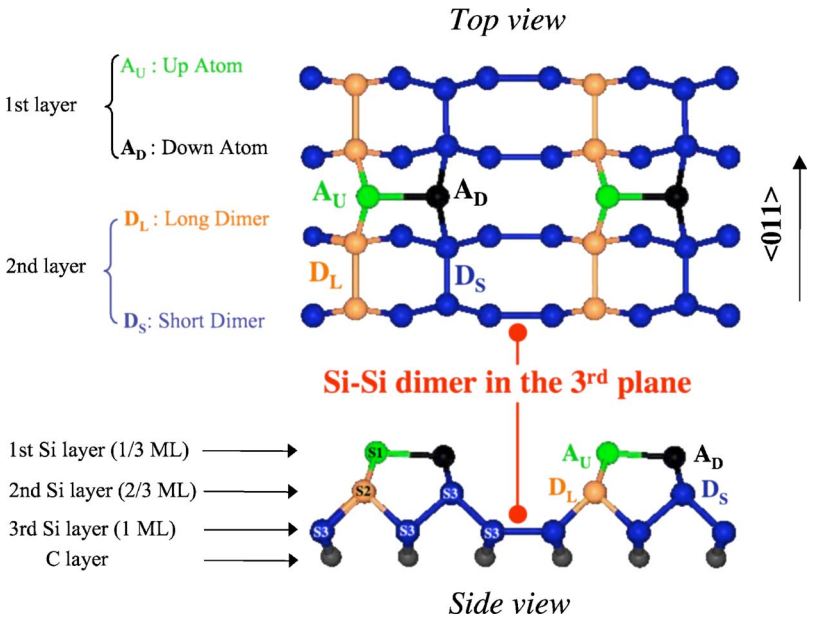

FIG. 1. (Color online) Schematic side view model of the clean β-SiC(100) 3×2 (after Ref. 27), showing the assignment of the surface core-level shifts S1, S2, and S3 to the up (A_U) and down (A_D) atoms of the topmost Si dimer in the first atomic plane, to the dimer long D_L and dimer short D_S in the second atomic plane, and to the atoms and dimer in the third atomic plane.

significant Si to C charge transfer leading to a polar (100) surface for cubic β-SiC.[24,25] Also, a large lattice mismatch with corresponding silicon (−20%) and diamond (+22%), together with strain, has been shown to significantly influence the surface structure.[24,25] The complex structure of Si-rich 3×2 reconstruction has been determined only recently by real-space atom-resolved STM,[26] synchrotron radiation-based grazing incidence x-ray diffraction[27] (GIXRD), and photoelectron diffraction[28] (PED) experimental techniques and by *ab initio* total energy pseudopotential calculations.[29] The morphology of the 3×2 surface reconstruction includes three Si atomic layers [1/3+2/3+1 Si ML (monolayer)] on top of the first carbon plane.[27–29] The topmost layer is made of asymmetric Si dimers all tilted in the same direction forming rows in a 3×2 array as identified by real space atom-resolved STM experiments[26] and confirmed by *ab initio* calculations, GIXRD, and PED (Refs. 27–29) that provided a complete atomic structural model. The second layer is formed of Si-dimer rows having alternating long and short dimers (ALSDs) within a row,[27,28] while the third Si layer which also includes Si dimers is still part of the reconstruction since Si atomic positions are still slightly away from the bulk ones.[27,28] This gives a three adlayer asymmetric dimer (TAAD) model combined with alternating long and short dimers in the second plane (ALSD).[27–29] The atomic model of the β-SiC(100) 3×2 surface structure is given in Fig. 1.

Despite its fundamental and applied interests, there has been so far very few investigations only on the H interaction on cubic silicon carbide. It includes (i) a theoretical study devoted to the Si-terminated β-SiC(100) 2×1 surface,[30] (ii) atom-resolved STM and angle-resolved ultraviolet photoemission measurements, both for the Si-terminated $c(4\times2)/2\times1$,[8,31] and (iv) core-level and valence band photoemission experiments for the Si-rich β-SiC(100) 3×2 surface.[32]

Recently, a novel and particularly interesting feature of atomic hydrogen interaction has been discovered on a silicon carbide surface with the first H-induced semiconductor surface metallization.[33–35] Such a finding has been shown for the Si-rich β-SiC(100) 3×2 surface reconstruction using several experimental techniques with (i) band-gap closing in the I/V characteristics by scanning tunneling spectroscopy (STS), (ii) Fermi level buildup by valence band ultraviolet photoemission spectroscopy (UPS), and (iii) specific spectral features in multiple reflection-infrared absorption spectroscopy (MR-IRAS).[33] The H atoms were shown to terminate the topmost surface Si dangling bond by atom-resolved STM, UPS, and MR-IRAS.[33] The metallization process was interpreted in terms of H-induced specific defects occurring from an asymmetric attack of the Si–Si dimers located in the third atomic layer below the surface, leading to have only one Si dangling bond decorated by a H-atom.[33] Indeed, due to space limitation, the other Si dangling bond remains empty.[33] Most interestingly, such a H-induced metallization also occurs on the preoxidized 3×2 surface.[36] The H/β-SiC(100) 3×2 system has then been investigated by several *ab initio* total energy theoretical calculations also favoring H-induced surface metallization.[37–40] They predict H atoms terminating surface dangling bonds and interacting with the third Si atomic plane, in agreement with the experimental results.[33] However, a bridge-bond position is favored for H atoms in the third Si plane[37–40] versus H-induced dangling bond.[33] Synchrotron radiation-based core-level photoemission spectroscopy is a very appropriate tool to probe the changes occurring upon H atom interacting with surface and subsurface regions, in particular, exploring charge transfer leading to the metallization process.

In this article, we investigate the interaction of H atoms with the β-SiC(100) 3×2 surface by synchrotron radiation-based core-level photoemission spectroscopy at Si $2p$. The H atoms are found to induce significant charge transfer to the three Si atomic layers of the surface and subsurface. In addition, the H interaction leads to a large reactive component supporting an asymmetric charge transfer in the third atomic plane below the surface, leaving two Si atoms with a very different electronic status.

II. EXPERIMENTAL DETAILS

The angle-integrated photoemission experiments are performed on the VUV beamline at the synchrotron radiation facility in Trieste, Italy using the 2 GeV Elettra Sincrotrone storage ring. The photoelectron energy is analyzed with an angle-integrating hemispherical electrostatic analyzer having a total electron acceptance angle of ±8°. The overall energy resolution (analyzer+monochromator) at room temperature is better than 80 meV in the photon energy range from 114 to 150 eV used for the Si 2*p* core level. The Fermi level position is obtained from the Ta sample holder. In addition, we also use Si 2*p* constant initial state (CIS) measurements that have been performed at the Advanced Light Source (Berkeley) on the 7.0.1 beamline using an angle-resolving electron analyzer having an acceptance angle of ±1°.[28] Single domain β-SiC(100) single crystal thin film samples are prepared at CNRS-CRHEA (Sophia Antipolis, France) on a 4° vicinal Si(100) surface by chemical vapor deposition (CVD) leading to the formation of a SiC thin film with a thickness of about 1 μm. The native oxides, amorphous carbon (coming from the CVD process), and other impurities are removed from the surface of the "as received" SiC sample by sequences of thermal annealings up to 1250 °C, leading to a Si depletion at the surface and leaving a C-rich surface. Then, the surface stoichiometry is restored by appropriate cycles of Si deposition followed by thermal annealing resulting in the formation of a perfect single domain 3×2 surface reconstruction.[24–28] The surface ordering is checked by low energy electron diffraction to give sharp single domain 3×2 patterns. Atomic H exposures are performed at 300 °C using high purity research grade molecular H_2 dissociated by a heated tungsten filament at a H_2 pressure of 1.10^{-6} torr in the vacuum chamber. In order to avoid contamination, we use a very rigorous experimental protocol, including intensively baked gas line (for H_2 exposures) and outgassed tungsten filament (well known to desorb, e.g., CO). The β-SiC(100) sample and the Si source are very carefully outgassed to prevent contaminant deposition and reaction on the surface. The Si deposition and/or β-SiC(100) sample thermal annealing are always performed in the low 10^{-10} torr. Additional information about other experimental details and high quality SiC surface preparation can be found elsewhere.[23–28,33,36]

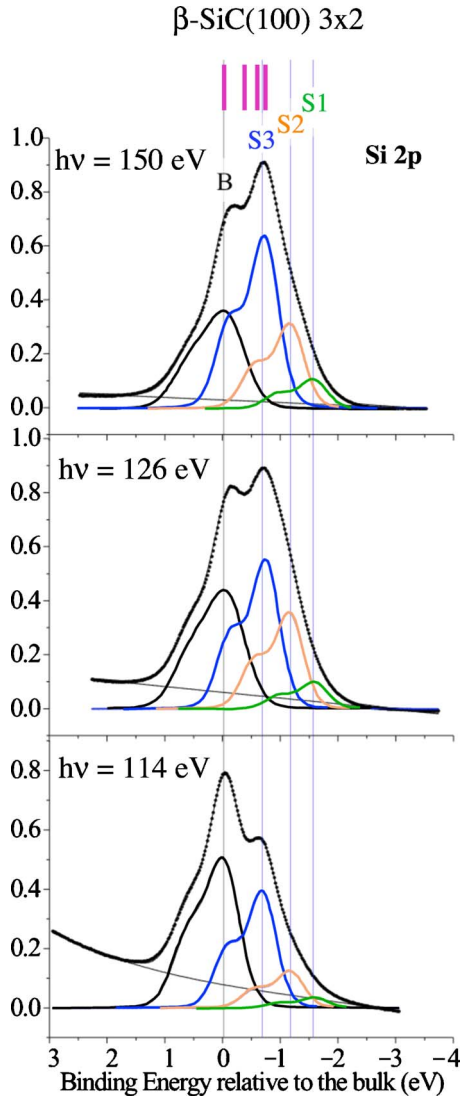

FIG. 2. (Color online) Si 2*p* core-level spectra with peak decomposition into bulk (B) and surface shifted (S1, S2 and S3) components for the clean β-SiC(100) 3×2 surface reconstruction at photon energies of $h\nu$=150 eV (surface sensitive), 126 eV, and 114 eV (bulk sensitive). The binding energy (BE) scale is relative to the bulk B component. The four bars located at the top of the figure mark the calculated surface core-level shifts at +0.08, −0.28 and −0.3, −0.56, and −0.65 eV binding energy, respectively, taken from Ref. 29 with the 0.28 and −0.3 eV components that are very close in energy being represented by one bar only.

III. RESULTS

A. Si 2*p* core level for the clean β-SiC(100) 3×2 surface

We first look at the Si 2*p* core-level peak fitting for the clean β-SiC(100) 3×2 surface to discriminate between bulk, surface, and subsurface shifted components. The Si 2*p* core-level spectra measured on the clean 3×2 reconstruction are shown in Fig. 2 for different photon energies. There is a large change in the Si 2*p* line shape when the photon energy varies between 114 and 150 eV. The change is due to the decrease of the inelastic mean free path with the photon energy (due to the concomitant variation of electron kinetic energy), because for 150 eV, the most surface sensitive spectra are recorded. The possible role of photoelectron diffraction effects is analyzed below. The background function was determined as part of the fit and selected as being the best polynomial function. Using a standard least-squares-fitting procedure, the spectra are decomposed into components consisting of spin-orbit split Voigt functions. A consistent fitting of the different spectra requires four different components: The bulk component B and three surface components S1, S2, and S3 that are, respectively, shifted by −1.4, −1.1, and −0.7 eV relatively to the bulk B component [Table I(a)]. A Lorentzian width of 85 meV and a spin-orbit splitting of 602 meV are used for all components, whereas the Gaussian widths are 600 meV for the bulk component B and 440 meV for the S1, S2, and S3 surface components, in agreement with previous studies on cubic silicon carbide.[41–43] Contrary to an earlier Si 2*p* core-level peak decomposition performed

TABLE I. (a) Binding energy E_b relative to the bulk (B) in eV of the Si $2p$ surface core-level shifted (S1, S2, and S3) and reacted (R) components for the clean and atomic H exposed β-SiC(100) 3×2 surfaces. (b) ΔE_b binding energy shifts of the Si $2p$ surface core-level S1, S2, and S3 components upon various atomic H exposures of the β-SiC(100) 3×2 surface from 20 to 60 L.

(a)	E_b (eV)	Clean	20 L of H	40 L of H	60 L of H
	S1	−1.4	−1.7	−1.95	−2
	S2	−1.1	−1.25	−1.4	−1.4
	S3	−0.7	−0.87	−0.93	−1
	R	N/A	−0.45	−0.48	−0.53
(b)	ΔE_b (eV)		20 L of H	40 L of H	60 L of H
	S1		−0.3	−0.55	−0.6
	S2		−0.15	−0.3	−0.3
	S3		−0.17	−0.23	−0.3

for this 3×2 surface reconstruction in the framework of the double dimer row model,[41] no additional component related to surface defects is needed at the lower binding energy side to account for the present core-level shapes. Our core-level peak decomposition into three surface shifted components (S1, S2, and S3) is also in excellent agreement with other results based on room and low temperatures Si $2p$ core-level photoemission experiments performed at Advanced Light Source (Berkeley)[28,44] and LURE (Orsay)[45] synchrotron facilities.

In order to explore the possible role of diffraction effects, we analyze in the following the Si $2p$ line shape modifications when the photon energy is changed. To quantify the contribution of photoelectron diffraction effects, we have performed CIS measurements for photon energies ranging from 150 eV (surface sensitive) to 480 eV (bulk sensitive). Since we used for these experiments an angle-resolved analyzer collecting photoelectrons within an acceptance angle of ±1°, the photoelectron diffraction effects are significantly enhanced when compared to the angle-integrated detector used for the data in Fig. 2 and actually have been used in determining the clean β-SiC(100) 3×2 surface structure.[28] Figure 3 shows the area of the different components normalized to the total area of the Si $2p$ core level. The purpose of this normalization is to determine the importance of photoelectron diffraction effects and to evaluate to which extent they affect the different components. We follow the intensity dependence of the bulk B and surface S2 and S3 components versus the photon energy. Since S1 has a weak intensity, it is not considered here. Several features can be clearly seen in Fig. 3. First, there are intensity oscillations due to photoelectron diffraction effects, but the maximum oscillation represents less than 15% of the total signal. Second, the oscillations are similar in the surface component S3 and in the bulk component B. S2 is fairly constant for the whole range of photon energies. Finally, the relative area of the bulk component B is enhanced when bulk sensitivity is higher, while the relative area of the surface component exhibits the opposite behavior. We can therefore conclude that photoelectron diffraction effects are behind the fast oscillations of the signals, while the smooth intensity changes observed in Fig. 3, which lead to a change of the intensities of S3 and B by a factor of 2, are due to the dependence of the inelastic mean free path on the electron kinetic energy. Furthermore, since for a 150 eV photon energy the inelastic mean free path for Si $2p$ photoelectrons is minimum, the surface components should decrease when going from 150 to 114 eV, as indeed observed above in Fig. 1 and also in Ref. 41.

We can now safely interpret the above decomposition in the frame of the TAAD-ALSD structural model of the 3×2 surface reconstruction recently derived from GIXRD and PED measurements, atom-resolved STM experiments, and *ab initio* total energy theoretical calculations, which is described above.[26–29] This structure includes three Si atomic planes of, respectively, 1/3, 2/3, and 1 ML coverages. The

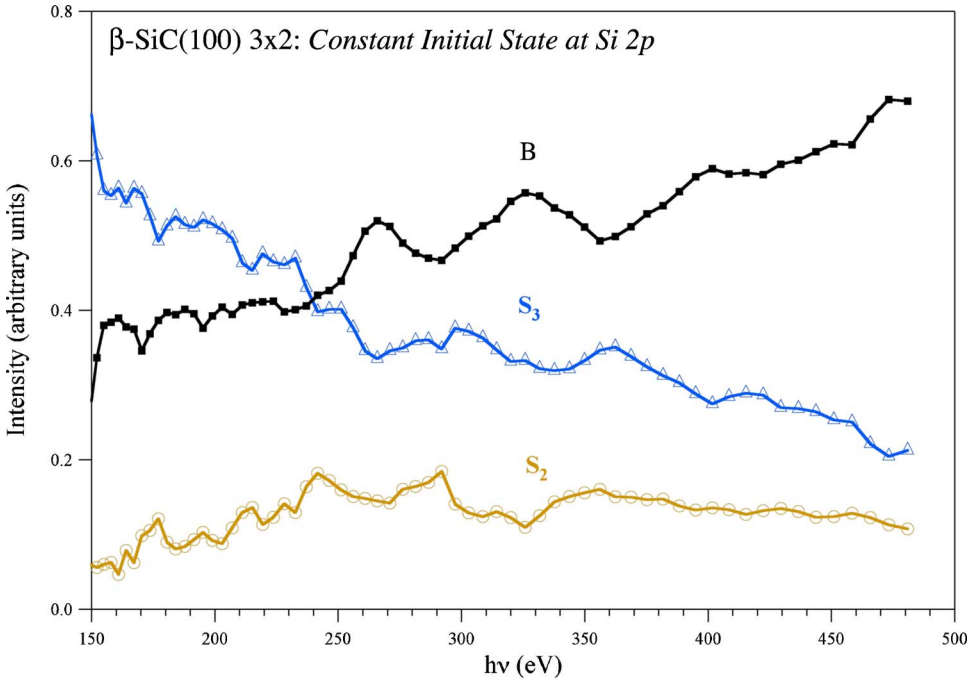

FIG. 3. (Color online) Si $2p$ core-level constant initial state (CIS) spectra for the bulk B and surface shifted S2 and S3 components for the clean β-SiC(100) 3×2 surface at photon energy ranging from $h\nu$=150 eV (surface sensitive) to $h\nu$=480 eV (bulk sensitive). The integral intensities of S2, S3, and B components are normalized to the total integral intensity of the whole spectrum.

Si ad-dimers of the topmost layer are asymmetric, while alternating long and short Si dimers (ALSDs) of the second layer are connected, respectively, to the up atom A_U and the down atom A_D of the asymmetric ad-dimer. Charge transfer occurs from the down atom toward the up atom within the asymmetric ad-dimer and is expected to also affect the short dimer of the second layer that is connected to the down atom of the ad-dimer. One should also note that the Si atoms belonging to the third layer may also be affected by a charge transfer toward the C atoms of the underlying atomic plane. Therefore, we propose to assign the three resolved surface components as follows: The S1 component at the lowest −1.4 eV binding energy is related to the up atom of the ad-dimer; the S2 component at −1.1 eV binding energy corresponds to the long dimer connected to the previous up atom; and finally, the S3 component at −0.7 eV involves both the short dimer of the second plane and the Si atoms of the third atomic plane, since the charge transfer that they encounter may be close enough so that they participate to the same component. As far as the down atom of the ad-dimer is concerned, it may contribute to the bulk component, as a result of the strong charge transfer toward the up atom. These assignments are in qualitative agreement with theoretical *ab initio* calculations of the surface core-level shifts performed for the TAAD model[29] including five surface shifted components at +0.08, −0.28, −0.3, −0.56, and −0.65 eV binding energies corresponding, respectively, to (i) the down atom, (ii) the dimer connected to the latter (located in the second plane and corresponding to the short dimer identified by GIXRD), (iii) the atoms in the third plane, (iv) the dimer (corresponding to the long dimer identified by GIXRD) located in the second plane and connected to the A_U up atom, and (v) the A_U up atom of the topmost asymmetric dimer.[27] Taking into account the physical broadening of the Si $2p$ core level for SiC, these five components reduce to three, whereas the quantitative discrepancy between experimental and theoretical binding energies may primarily result from the limits of the calculation method itself. At a 150 eV photon energy, the intensity ratio between the surface components is 1:3:6, which can be compared to the number of atoms involved in each component (1:2:8), the difference possibly resulting from either small photoelectron diffraction effects that cannot be totally neglected with a photoelectron collection angle of ±8° and/or attenuation of the third layer signal by the two topmost Si layers. One can see in Fig. 1 the top and side view schematics of the β-SiC(100) 3×2 surface reconstruction with the above assignment of the Si $2p$ surface core-level shifted components to the atoms involved in the reconstruction.

B. Si 2*p* core-level for the H-covered β-SiC(100) 3×2 surface

We now follow the effect of hydrogen atoms interaction on the β-SiC(100) 3×2 surface and subsurface regions looking at the Si $2p$ core-level changes. We first explore possible charge transfers induced by the hydrogen atoms looking at the binding energy changes of the S1, S2, and S3 surface and subsurface shifted components. Therefore, we

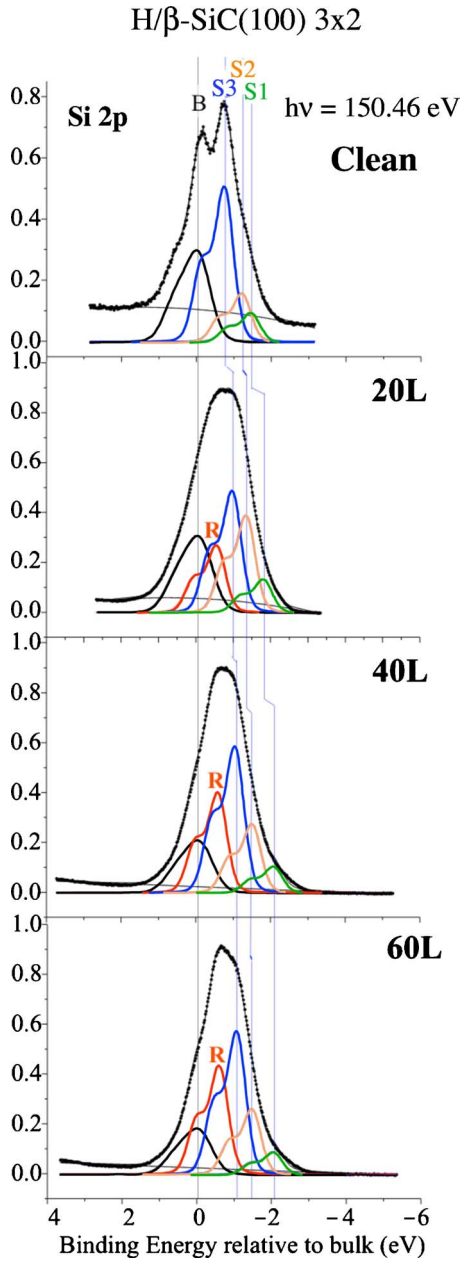

FIG. 4. (Color online) Si $2p$ core-level spectra with peak decomposition (B, S1, S2, S3, and a new reactive R component) for clean β-SiC(100) 3×2 and atomic hydrogen exposed (from 20 to 60 L) surfaces. All the spectra are aligned on the bulk B component taken as the origin of the relative binding energy (BE) scale. The photon energy is 150.46 eV.

turn to the curve fitting procedure of the core-level spectra for the H exposed surfaces using the same Lorentzian and Gaussian widths as the ones used for the clean surface. Figure 4 displays the Si $2p$ core-level spectra measured at the very surface sensitive photon energy of 150.46 eV for the clean and hydrogen-covered β-SiC(100) 3×2 surfaces after successive atomic hydrogen exposures ranging from 20 to 60 L (1 L$=10^{-6}$ torr s). Notice that, at this photon energy, we are probing ≈5 atomic layers including the three top-surface Si planes, the first C plane (fourth layer), and the first bulk Si plane (fifth layer)—see Fig. 1. The Si $2p$ core-level spectra are presented with a relative binding energy scale in order to facilitate the identification of binding energy

shifts. One should also remark that the Si 2*p* core level for the clean surface in Fig. 4 shows the S1 and S2 surface components at a 0.2 eV smaller binding energy compared to the corresponding spectrum in Fig. 1. This is due to the fact that the two surfaces do not have exactly the same Si coverage, with a slightly larger one for the latter (Fig. 1). Indeed, the β-SiC(100) surface can reconstruct 3×2 with different Si thicknesses, leading to having the same surface shifted component S1 and S2 but different relative intensities and also slightly different binding energies as previously observed.[46] One feature of interest is the behavior of the S1, S2, and S3 surface shifted components upon H atom interaction. As can be seen from Fig. 4, these surface components are shifted toward the lower binding energy side by rather large values reaching −0.6, −0.3, and −0.3 eV energy shifts for the S1, S2, and S3 components, respectively, at 60 L H exposure when compared to the clean 3×2 surface. Such a behavior clearly indicates a global charge transfer to the atoms of the three first Si atomic planes, in excellent agreement with a picture of H-induced surface metallization.[33] Table I(a) gives the binding energies E_b relative to the bulk B component of the Si 2*p* S1, S2, and S3 surface core level shifted components for 20, 40, and 60 L H exposures, while Table I(b) displays the binding energy shifts ΔE_b occurring upon the same H exposures for the S1, S2, and S3 surface components. Interestingly, such large energy shifts to lower binding energy are also observed in the case of metal-induced semiconductor surface metallization,[47,48] in particular, with alkali metals which also belong to the group I elements of the Mendeleev classification.[49–55]

Another important feature of interest is a new reactive component showing up at the Si 2*p* core level upon hydrogen interaction with the β-SiC(100) 3×2 surface reconstruction at the lowest H exposure as seen in Fig. 4. Indeed, we observe that the Si 2*p* core-level spectra are broadened upon increasing H exposures with a saturation occurring between 40 and 60 L. This broadening results from the emergence of a new reactive chemical component (labeled R) showing already after the first hydrogen exposure at 20 L. R is located between the bulk B and the surface S3 components with a binding energy relative to the bulk varying from −0.45 to −0.53 eV (depending on the hydrogen exposure), while S3 is now shifted by −1 eV relative to the bulk component B [see Table I(a)]. The reactive component R is very likely derived from the S3 component. It clearly suggests that H atom interaction results in asymmetric charge transfer in the subsurface region. Indeed, such a situation could be consistent with the proposed H-induced asymmetric attack of the Si dimer located in the third Si plane, resulting in dimer breaking that leaves two dangling bonds with, due to steric hindrance, only one of them being decorated with a hydrogen atom.[33] In such a scenario, the two Si atoms forming this Si–Si dimer (in the third plane) on the clean β-SiC(100) 3×2 surface prior to hydrogenation would have a very different electronic status on the hydrogenated one.[33] In this case, this would explain the large difference in binding energy (0.47 eV, Table I) between the H-terminated and empty dangling bonds resulting from the asymmetric attack of the Si dimer located in the third Si atomic plan (see Fig. 3).

Another effect could also possibly contribute to the R component. Indeed, as mentioned above, the B component is the sum of two contributions, the bulk atoms and the down atoms of the ad-dimer (see Fig. 3). Actually, the down atom A_D of the topmost ad-dimer is very likely to also participate, at least in part, to the reactive R component showing upon H exposure since the observed energy for R at −0.53 eV shift from the bulk B component is comparable to the −0.6 eV shift of the S1 component related to the A_U up atom. In turn, this would somehow affect the intensities of the bulk B component, and also of the reactive R component. So, the new R component showing upon H interaction would result not only from bond breaking in the third Si plane but also from the shift of the surface component related to the down atom (in the first Si plane), leading to having its contribution separated from the bulk B component. However, keeping in mind the small intensity of the shifted component S1 related to the up atom (first Si plane),[56] the contribution of the hydrogenated down atom to the reacted R component is likely to remain rather marginal. This means that, primarily, the Si-dimer bond breaking occurring in the third atomic plane would be the dominant contribution to the reacted R component.

One can also explore possible band-bending effects resulting from the H interaction with the surface, tracking rigid kinetic energy shifts of the Si 2*p* bulk component upon atomic hydrogen exposures, despite the fact that the SiC sample exact doping is not known. Using a kinetic energy scale, Fig. 5 displays the Si 2*p* core-level spectra measured at a photon energy of 150.46 eV (surface sensitive), for the clean and hydrogen-covered β-SiC(100) 3×2 surfaces for the same H exposure sequence as in Fig. 4. We look at the behavior of the bulk B component, which is of special interest. Indeed, upon atomic H exposures, one can see that the latter is shifted to the lower kinetic energy side starting at −0.16 eV for an initial 20 L of H exposure and reaching very large values at −0.73 and −0.84 eV for 40 and 60 L of H exposures, respectively. Such a behavior indicates band bending in agreement with the H-induced surface metallization.[33] It is very interesting to remark that such large band-bending effects are comparable to those observed with alkali metals, in particular, on III-V compound semiconductor surfaces.[49–53]

IV. DISCUSSION

Our above synchrotron radiation-based core-level photoemission spectroscopy experiments bring a deeper knowledge and understanding about the H atom interaction with the β-SiC(100) 3×2 surface reconstruction that led to the recent discovery of the first H-induced semiconductor surface metallization.[33] It clearly supports a picture of H-induced charge transfer to the surface and subsurface regions as evidenced through the behavior of the three Si 2*p* core-level surface components shifted to lower binding energy. Indeed, this shows that the charge transfer and therefore the subsequent metallization process affect the three Si atomic planes of the 3×2 surface reconstruction. In addition, together with the existence of a specific IRAS vibration

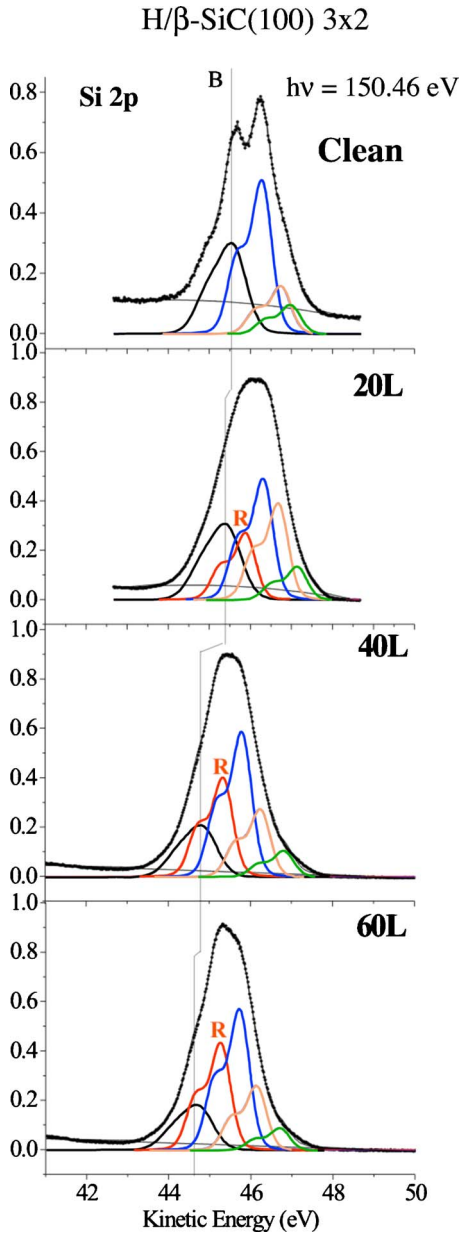

FIG. 5. (Color online) Si 2*p* core-level spectra with peak decomposition for clean β-SiC(100) 3×2 and atomic hydrogen exposed (from 20 to 60 L) surfaces. The kinetic energy scale is relative to the bulk B component on the clean surface. The photon energy is 150.46 eV.

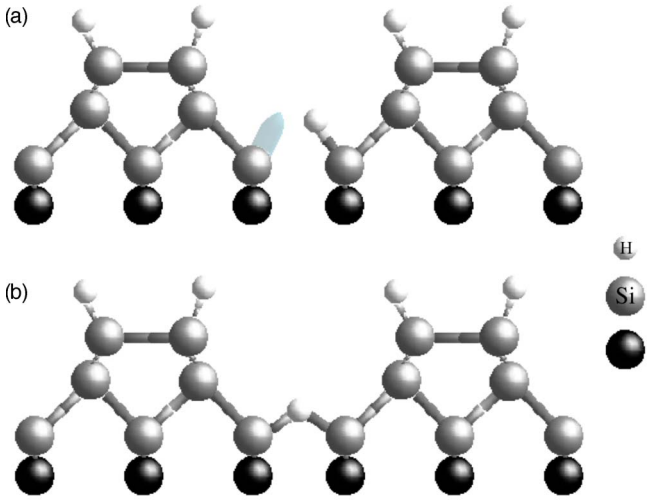

FIG. 6. (Color online) (a) Atomic side view model of asymmetric charge transfer for the H atom interaction with the β-SiC(100) 3×2 surface with an asymmetric attack on the Si–Si dimers located in the third plane with, due to steric hindrance, only one Si dangling bond being decorated by a H atom as proposed in Ref. 33. (b) Atomic side view model of the H/β-SiC(100)3×2 surface as proposed by *ab initio* total energy calculations (Refs. 37–40) with the H atom located in the third plane in a bridge-bond position.

mode,[33,57,58] the occurrence of a R reacted component indicates an asymmetric charge transfer taking place in the third atomic plane. This would favor a picture of bond breaking taking place below the surface as proposed [Fig. 6(a)] on the ground of previous experimental results[33] versus a model of bridge-bond position for the H atom [Fig. 6(b)], as suggested in recent *ab initio* calculations.[37–40] In such a situation, this leaves a H terminating a Si dangling bond and, due to steric hindrance, a dangling bond defect. In this case, a bond breaking could occur either in the second or the third Si atomic plane below the surface. Since IRAS measurements show a clear vibration mode at 2140 cm^{-1} that indicates a H atom terminating a Si dangling bond belonging to an atom located above and bonded to the C plane,[33,57,58] the R component can be interpreted in terms of Si–Si dimers breaking in the third plane.[33,58] The Si–Si distance in the dimer has been measured to be 2.38 ± 0.02 Å by GIXRD (Ref. 27) and 2.43 ± 0.10 Å by PED (Ref. 28) and calculated at 2.41 Å,[29] i.e., the same distance at $\approx$2.40 Å within the error bars. One can therefore easily imagine that, within such a limited space, it is difficult to accommodate two H atoms, one on each of the dangling bond resulting from Si-dimer breaking. Only one of these two Si dangling bonds could be decorated with a hydrogen atom, leading to a dangling bond defect formation.[33] Therefore, it is likely that the H-induced asymmetric attack on the third plane dimers also influences the electronic status of the overall reconstruction. In fact, the electron belonging to the other Si atom and initially involved into the Si–Si dimer bonding could possibly be transferred, at least in part, to the underlying C atoms since the carbon plane has a higher electron affinity at 2.55 compared to silicon (1.9). Indeed, this has been recently shown in the deuterium-induced metallization of the same β-SiC(100) 3×2 surface, with a larger charge transfer to the carbon plane (as identified at the C 1*s* core level) compared to the Si planes.[59] Incidentally, such a charge transfer to the C plane is also observed for the preoxidized surface metallized by H.[36] Therefore, the asymmetric charge transfer initiated in the third atomic layer is likely to trigger the H-induced surface metallization process in addition to the charge transfer resulting from H atoms terminating topmost surface dangling bonds. Furthermore, since the β-SiC(100) 3×2 is a polar surface, an asymmetric charge transfer in the third Si atomic plane further supports the involvement of the first C atomic plane located just below as mentioned just above (see Fig. 1). Also, the fact that the metallization induced by hydrogen could be traced by scanning tunneling spectroscopy[25,33] further supports a picture of the topmost atomic plane to be also involved in this process. Indeed, in addition to the large shifts to lower binding energy of the Si 2*p* surface S1, S2,

and S3 components indicating a large charge transfer to the surface atoms upon H interaction, the latter quenches the electronic surface state (related to the Si–Si dimers) located at 1.5 eV below the Fermi level.[33] This supports a more ionic type of H–SiC bonding, rather similar to the behavior of alkali metals on compound III-V semiconductors. However, it is in contrast with alkali metal interaction with elemental group IV semiconductors as Si(100) 2×1, where the electronic surface state is not destroyed but shifted to higher binding energy, indicating a polarized covalent bonding.[60]

We now explore the possible origin of the large band bending taking place during the β-SiC(100) 3×2 surface hydrogenation (up to −0.84 eV at 60 L of H, compared to the clean surface). Such a band bending could result either from defects and/or from hydrogen-induced gap surface states.[47–53] Here, one can notice that the hydrogen atom interaction with the β-SiC(100) 3×2 surface could be interpreted in terms of a specific dangling bond defect in the third plane (related to the asymmetric attack occurring at the Si dimers and also identified by the R reacted component in Fig. 4) as suggested above.[33] This makes the H/β-SiC(100) 3×2 "interface" a "reactive one." This situation could be understood when comparing to reactive metal/semiconductor interfaces for which the Fermi level position is pinned by defects.[47,48,52] Therefore, it is reasonable to think that a H-induced specific defect below the surface in the third atomic plane[33] could be responsible, at least in part, for the large band bending observed here. However, the H (D) interaction β-SiC(100) 3×2 surface also results in electronic states created in the band gap near the Fermi level with a Fermi step indicating surface metallization as evidenced by valence band photoemission spectroscopy.[25,33–36,59] These electronic surface states could possibly act as "metal-induced" gap states (as for metal/semiconductor interfaces), leading also to the Fermi level pinning and to the observed band bending. Again, it is not possible at this point to discriminate between these two mechanisms and evaluate further their relative importance since our SiC sample exact doping is not known. Anyway, the observed band bending is not large enough to move the Fermi level position out of the band gap into the conduction band as observed, e.g., for some small band-gap semiconductor/metal interface.[53]

It is now appropriate to correlate our present and previous[33] experimental results with several very recent *ab initio* total energy local density functional calculations on atomic hydrogen interaction with the β-SiC(100) 3×2.[37–40] Interestingly enough, all the latter also conclude to H-induced surface metallization with H atoms (i) also terminating the topmost surface Si dangling bonds and (ii) interacting with Si atoms located in the third Si atomic plane, in excellent agreement with real-space atom-resolved STM, UPS, and MR-IRAS experimental results.[33] However, as first reported by di Felice *et al.*[37] and then supported by three other theoretical studies,[38–40] an alternative geometry is suggested for the H atom bonding configuration in the third Si plane with H atom located in a bridge-bond adsorption site between two Si atoms belonging to the same Si dimer as depicted in Fig. 6(b). The latter is found to have a lower energy compared to H terminating a Si dangling bond.[37–40] At this point, let us emphasize that such a model of bridge-bond position for H atoms is clearly not consistent from its own with the above experimental results. Indeed, in such a situation, the two Si atoms bonded to same H atom would have the same electronic status and therefore no reactive component would show at the Si 2*p* core level (Figs. 4 and 5). Here, one has to consider that the difference may come from the fact that these theoretical investigations are "0 K" calculations while experimentally, H exposures are performed on a surface maintained at 573 K, with the data acquisition performed at room temperature for the H-covered surface.[33] These are, of course, very different situations. Therefore, it is somewhat difficult to compare predictions based on calculations not taking into account the entropy and performed for a "frozen" system. While such "static" calculations are very useful and confirm the surface metallization by hydrogen, they certainly cannot address complex issues such as dynamical processes likely occurring here during H interaction[59] and safely derive information about the latter. While one can think that, at 0 K, the model proposed by these *ab initio* total energy calculations with the H atom in a bridge-bond position in the third Si plane is reasonable,[37–40] the situation is likely to be very different at room or elevated temperatures. Our above results are clearly not consistent with a "symmetric" bridge-bond position as predicted by the *ab initio* 0 K calculations, since the proposed bridge-bond model is very unlikely to exhibit an asymmetric charge transfer behavior,[37–40] like the model of H-induced asymmetric attack on the third plane Si dimer.[33] So, while the latter model is favored by the present core-level photoemission study, one cannot exclude other possible bonding configurations that could also lead to an asymmetric charge transfer. In addition, it is possible to imagine a dynamical situation occurring at room temperature in the third atomic plane with, e.g., H atoms hopping from one dangling bond to another one or a flipping between H atom terminating one of the dangling bond[33] and H in a bridge-bond position.[37–40] A bridge-bond position for the H atom in the third Si plane is, however, possible but would require very low temperature experiments not easy to carry out using electron related techniques likely to result in frozen carriers on a wide band-gap semiconductor and subsequent charging effects. Clearly, additional experimental and theoretical investigations are needed to explore further the occurrence of such a mechanism.

Another feature of interest in two of these theoretical works is the calculation of surface vibrational modes.[39,40] For the proposed Si–H–Si bridge-bond configuration in the third Si plane, the vibration frequency has been predicted to be around 1100 cm^{-1} in Ref. 39 and 1410 or 1450 cm^{-1} in Ref. 40. In addition, the latter calculation also finds a 1374 cm^{-1} mode assigned to a Si–H–Si bridge-bond configuration in the second Si plane.[40] Clearly, none of these modes related to H atoms in a bridge-bond position have been observed in the MR-IRAS experiments, which exhibit a flat response in the corresponding spectral range.[33] Instead, the 2140 cm^{-1} wavenumber found experimentally[33] is assigned to a H–Si mode in Ref. 39 but is not found in Ref. 40. The 2140 cm^{-1} observed in infrared absorption spectroscopy has been as-

signed to a H atom terminating a Si dangling located above the C plane.[33,57,58] Indeed, such a mode could also be identified in similar IRAS experiments performed on hydrogen atoms covering the Si-terminated β-SiC(100) $c(4\times2)$ surface reconstruction[58] where the topmost Si plane is located just above the first carbon plane.[25,56,61] This further supports the assignment of the vibration modes around 2140 cm^{-1} to be related to H–Si–C configuration only, not to a H–Si–Si one, while the 2118 cm^{-1} mode observed experimentally is related to the H–Si–Si vibration mode for H atoms terminating the topmost surface dangling bonds.[33,58]

Turning to the metallization process, the above Si $2p$ results indicate that it is likely to result from two origins: (i) An effective charge transfer from H atoms terminating each topmost Si dangling bond belonging to the first Si atomic plane and (ii) an attack in the third Si plane leading to an additional asymmetric charge transfer. It is interesting to correlate the present results and model to the recent evidence that H also metallizes the ZnO$(10\bar{1}0)$ surface.[62] Interestingly enough, the latter behavior is found to take place also in case of an asymmetric charge transfer, i.e., when a H atom terminates only one of the two dangling bonds belonging to the topmost surface dimer, with no metallization taking place when the two dangling bonds are H terminated. Also, notice that a similar asymmetric charge transfer also occurs when H atoms are selectively removed by STM-induced H atom electronic desorption, creating dangling bond lines predicted to have a conducting one-dimensional metallic character.[10–17]

V. CONCLUSIONS

In conclusion, we have studied the interaction of atomic H with the Si-rich β-SiC(100) 3×2 surface by Si $2p$ core-level photoemission spectroscopy using synchrotron radiation. This investigation brings deeper insights into the understanding of H-induced metallization of a semiconductor surface, in particular, about the interatomic charge transfers occurring in the surface and subsurface regions. The results indicate that the H interaction leads to a significant charge transfer to the surface and subsurface atoms in the three topmost Si planes, with an asymmetric charge transfer taking place in the third Si atomic layer leaving the two Si atoms with a very different electronic status. Such a behavior results from H atoms terminating the topmost surface dangling bonds and from their interaction with the Si–Si dimer located in the third layer below the surface that leads to dangling bond defect formation, in excellent agreement with the picture proposed on the ground of STM/STS, UPS, and MR-IRAS experiments to account for the H-induced surface metallization. However, while a bridge-bond position in the third atomic plane as recently predicted by *ab initio* total energy "frozen" calculations is possible at very low temperatures, our results clearly do not favor such a model.

ACKNOWLEDGMENTS

The authors are grateful to the staff of the Elettra Sincrotrone, Trieste, and of the Advanced Light Source, Berkeley, for outstanding technical assistance. They want to thank J. D. Dennlinger, D. Dunham, and E. Rotenberg for the CIS experiments performed at ALS in the framework of Ref. 28 and A. Leycuras at the Centre de Recherche sur l'Hétéroépitaxie et ses Applications, CRHEA-CNRS (Sophia-Antipolis, France), for providing the high quality β-SiC(100) single crystal thin films that were used in this investigation. The authors also acknowledge discussions with F. Amy, Y. J. Chabal, and E. Wimmer. The Elettra work was supported by the EU program for user large-scale facilities, while the ALS complementary CIS measurements were supported by the US National Science Foundation to the Northern Illinois University, the Northern Illinois University Graduate School Funds, and by MEC and CAM (Spain) (FIS2005-00747, S-0505/PPQ/0316).

[1] K. Oura, V. G. Lifshits, A. A. Saranin, A. V. Zotov, and M. Katayama, Surf. Sci. Rep. **35**, 1 (1999).
[2] G. S. Higashi and Y. J. Chabal, in *Handbook of Silicon Wafer Cleaning Technology: Science, Technology and Applications*, edited by W. Kern (Noyes, Park Ridge, NJ, 1993), p. 433.
[3] J. J. Boland, Phys. Rev. Lett. **65**, 3325 (1990).
[4] J. J. Boland, Phys. Rev. Lett. **67**, 1539 (1991); Surf. Sci. **261**, 17 (1992).
[5] G. S. Higashi, Y. J. Chabal, G. W. Trucks, and K. Raghavachari, Appl. Phys. Lett. **56**, 656 (1990).
[6] Y. J. Chabal and K. Raghavachari, Phys. Rev. Lett. **54**, 1055 (1985).
[7] M. Schluter and M. L. Cohen, Phys. Rev. B **17**, 716 (1977).
[8] V. Derycke, P. Fonteneau, N. P. Pham, and P. Soukiassian, Phys. Rev. B **63**, R201305 (2001).
[9] X. Peng, P. Krüger, and J. Pollmann, Phys. Rev. B **75**, 073409 (2007).
[10] T.-C. Shen, C. Wang, G. C. Abeln, J. R. Tucker, J. W. Lyding, Ph. Avouris, and R. E. Walkup, Science **268**, 1590 (1995).
[11] E. T. Foley, A. F. Kam, J. W. Lyding, and Ph. Avouris, Phys. Rev. Lett. **80**, 1336 (1998).
[12] L. Soukiassian, A. J. Mayne, M. Carbone, and G. Dujardin, Phys. Rev. B **68**, 035303 (2003); Surf. Sci. **528**, 121 (2003).
[13] S. Watanabe, Y. A. Ono, T. Hashizume, Y. Wada, J. Yamauchi, and M. Tsukada, Phys. Rev. B **52**, 10768 (1995).
[14] S. Watanabe, Y. A. Ono, T. Hashizume, and Y. Wada, Phys. Rev. B **54**, R17308 (1996).
[15] T. Hitsoguchi, T. Hashizume, S. Heike, S. Watanabe, and Y. Wada, Jpn. J. Appl. Phys., Part 2 **36**, L361 (1997).
[16] P. Doumerge, L. Pizzagalli, C. Joachim, A. Altibelli, and A. Baratoff, Phys. Rev. B **59**, 15910 (1999).
[17] D. R. Bowler and A. J. Fisher, Phys. Rev. B **63**, 035310 (2001).
[18] *Silicon Carbide, A Review of Fundamental Questions and Applications to Current Device Technology*, edited by W. J. Choyke, H. M. Matsunami, and G. Pensl (Akademie-Verlag, Berlin, 1998), Vols. I and II, and references therein.
[19] *Wide Band Gap Semiconductors: Present Status, Future Prospects and Frontiers*, edited by P. Soukiassian, J. Phys. D 40: Applied Physics, pp. 6139–6478 (2007).
[20] IEEE Trans. Electron Devices **46**(3) (1999) special issue on silicon carbide electronic devices, and references therein.
[21] D. Nakamura, I. Gunjishima, S. Yamaguchi, T. Ito, A. Okamoto, H. Kondo, S. Onda, and K. Takatori, Nature (London) **430**, 1009 (2004).
[22] R. Madar, Nature (London) **430**, 974 (2004).
[23] V. M. Bermudez, Phys. Status Solidi B **202**, 447 (1997), and references therein.
[24] P. Soukiassian and F. Semond, J. Phys. IV **7**, 101 (1997); P. Soukiassian, Mater. Sci. Eng., B **61**, 506 (1999), and references therein.
[25] P. Soukiassian and H. Enriquez, J. Phys.: Condens. Matter **16**, S1611 (2004), special section on silicon carbide, and references therein.
[26] F. Semond, P. Soukiassian, A. Mayne, G. Dujardin, L. Douillard, and C. Jaussaud, Phys. Rev. Lett. **77**, 2013 (1996).
[27] M. D'angelo, H. Enriquez, V. Yu. Aristov, P. Soukiassian, G. Renaud, A. Barbier, M. Noblet, S. Chiang, and F. Semond, Phys. Rev. B **68**, 165321 (2003).
[28] A. Tejeda, D. Dunham, F. J. García de Abajo, J. D. Denlinger, E. Rotenberg, E. G. Michel, and P. Soukiassian, Phys. Rev. B **70**, 045317 (2004).
[29] W. Lu, P. Krüger, and J. Pollman, Phys. Rev. B **60**, 2495 (1999).
[30] B. I. Craig and P. V. Smith, Surf. Sci. **233**, 255 (1990); Physica B **170**, 518 (1991).

[31] S. M. Widstrand, L. S. O. Johansson, K. O. Magnusson, M. I. Larsson, H. W. Yeom, S. Hara, and S. Yoshida, Surf. Sci. **479**, 247 (2001).
[32] H. W. Yeom, I. Matsuda, Y. C. Chao, S. Hara, and R. I. G. Uhrberg, Phys. Rev. B **61**, R2417 (2000).
[33] V. Derycke, P. Soukiassian, F. Amy, Y. J. Chabal, M. D'angelo, H. Enriquez, and M. Silly, Nat. Mater. **2**, 253 (2003).
[34] M. Wilson, Phys. Today **56**(June), 18 (2003).
[35] V. M. Bermudez, Nat. Mater. **2**, 218 (2003).
[36] M. Silly, C. Radtke, H. Enriquez, P. Soukiassian, S. Gardonio, P. Moras, and P. Perfetti, Appl. Phys. Lett. **85**, 4893 (2004).
[37] R. di Felice, C. M. Bertoni, C. A. Pignedoli, and A. Catellani, Phys. Rev. Lett. **94**, 116103 (2005).
[38] F. de Brito Mota, V. B. Nascimento, and C. M. C. de Castilho, J. Phys.: Condens. Matter **17**, 4739 (2005); **18**, 7505 (2006).
[39] H. Chang, J. Wu, B.-L. Gu, F. Liu, and W. Duan, Phys. Rev. Lett. **95**, 196803 (2005).
[40] X. Peng, P. Krüger, and J. Pollmann, Phys. Rev. B **72**, 245320 (2005).
[41] H. W. Yeom, Y. C. Chao, S. Terada, S. Hara, S. Yoshida, and R. I. G. Uhrberg, Phys. Rev. B **56**, R15525 (1997).
[42] L. I. Johansson, F. Owman, and P. Martensson, Phys. Rev. B **53**, 13793 (1996).
[43] V. Yu. Aristov, H. Enriquez, V. Derycke, P. Soukiassian, G. Le Lay, C. Grupp, and A. Taleb-Ibrahimi, Phys. Rev. B **60**, 16553 (1999).
[44] D. Dunham, P. Soukiassian, E. Rotenberg, and J. D. Denlinger, (unpublished).
[45] V. Derycke, H. Enriquez, V. Yu. Aristov, P. Soukiassian, G. Le Lay, S. Grupp, and A. Taleb-Ibrahimi (unpublished).
[46] C. Radtke, H. Enriquez, J. Arnault, P. Soukiassian, P. Moras, C. Crotti, and P. Perfetti, Appl. Phys. Lett. **87**, 193110 (2005).
[47] L. Brillson, in *Handbook on Semiconductors*, 2nd ed., edited by P. T. Landsberg (Elsevier, Amsterdam 1992), Vol. 1, Chap. 8, and references therein.
[48] E. H. Rhoderick and R. H. Williams, *Metal-Semiconductor Contacts* (Clarendon, Oxford, 1988), and references therein.
[49] T. Kendelewicz, P. Soukiassian, M. H. Bakshi, Z. Hurych, I. Lindau, and W. E. Spicer, Phys. Rev. B **38**, 7568 (1988); J. Vac. Sci. Technol. B **6**, 1331 (1988).
[50] P. Soukiassian and T. Kendelewicz, *Metallization and Metal/Semiconductor Interfaces*, NATO Advance Study Institute, Series B: Physics (Plenum, New York, 1989), Vol. 195, p. 465.
[51] P. Soukiassian, *Fundamental Approach to New Materials Phases: Ordering at Surfaces and Interfaces*, Springer Series in Materials Science Vol. 17 (Springer, New York, 1992), p. 197.
[52] K. M. Schirm, P. Soukiassian, P. S. Mangat, and L. Soonckindt, Phys. Rev. B **49**, 5490 (1994).
[53] V. Yu. Aristov, G. Le Lay, P. Soukiassian, K. Hricovini, J. E. Bonnet, J. Oswald, and O. Olsson, Europhys. Lett. **26**, 359 (1994).
[54] P. S. Mangat and P. Soukiassian, Phys. Rev. B **52**, 12020 (1995).
[55] P. S. Mangat, P. Soukiassian, Y. Huttel, and Z. Hurych, J. Vac. Sci. Technol. B **12**, 2694 (1994).
[56] Similarly, for the β-SiC(100) $c(4\times2)$ surface reconstruction, the two Si $2p$ surface shifted components related to the up and down dimers located in the topmost Si layer have the same low intensity; see Ref. 43 and also A. Tejeda, E. Wimmer, P. Soukiassian, D. Dunham, E. Rotenberg, J. D. Denlinger, and E. G. Michel, Phys. Rev. B **75**, 195315 (2007).
[57] N. Sieber, T. Stark, Th. Seyller, L. Ley, C. A. Zorman, and M. Mehregany, Appl. Phys. Lett. **80**, 4726 (2002).
[58] F. Amy and Y. J. Chabal, J. Chem. Phys. **119**, 6201 (2003).
[59] J. Roy, V. Yu. Aristov,C. Radtke,P. Jaffrennou, H. Enriquez, P. Soukiassian, P. Moras, C. Spezzani, C. Crotti, and P. Perfetti, Appl. Phys. Lett. **89**, 042114 (2006).
[60] P. Soukiassian, M. H. Bakshi, Z. Hurych, and T. M. Gentle, Surf. Sci. Lett. **221**, L759 (1989).
[61] P. Soukiassian, F. Semond, L. Douillard, A. Mayne, G. Dujardin, L. Pizzagalli, and C. Joachim, Phys. Rev. Lett. **78**, 907 (1997).
[62] Y. Wang, B. Meyer, X. Yin, M. Kunat, D. Langenberg, F. Traeger, A. Birkner, and Ch. Wöll, Phys. Rev. Lett. **95**, 266104 (2005).